Single-phase catalysis for reductive etherification of diesel bioblendstocks

Glenn R. Hafenstine,[a] Nabila A. Huq,[a] Davis R. Conklin,[a] Matthew R. Wiatrowski,[a] Xiangchen Huo,[a] Qianying Guo,[b] Kinga A. Unocic,[b] and Derek R. Vardon[a]*

[a]National Renewable Energy Laboratory, 15013 Denver West Parkway, Golden, CO, United States
[b]Oak Ridge National Laboratory, 1 Bethel Valley Road, Oak Ridge, TN, United States
*Derek.Vardon@nrel.gov

Section S1: Experimental Methods

Catalyst synthesis and characterization

Ultra-high purity hydrogen gas (2000 psig, 99.999+%, Airgas), ultra-high purity helium gas (2200 psig, 99.9999+%, Airgas), ammonia gas (9.97% with balance helium, General Air), hydrogen gas (10.00% containing 0.0068% oxygen and balance argon, General Air) and carbon monoxide gas (10% with balance helium, General Air) were used as delivered for batch and flow reactions or chemisorption measurements. Palladium-on-activated-carbon (5 wt% Pd, Aldrich), 1-butanol (anhydrous, 99.8%, Aldrich), 4-heptanone (98+%, Aldrich), acetone (for HPLC, GC, and residue analysis, 99+%, Aldrich) ethanol (absolute, anhydrous, Pharmco), n-octanol (99+%, Aldrich), n-hexanol (98+%, Aldrich), phosphoric acid (85 wt%, Aldrich), 6-undecanone (98+%, TCI) and palladium nitrate dihydrate were used as received. Niobic acid hydrate (CBMM), niobium phosphate (CBMM), and titanium dioxide (Alfa Aesar) were calcinated at 400 °C before catalytic efficiency testing. Nonane (99+%, Aldrich) was used as received for internal standard in gas chromatography analysis.

Metal oxide supports were phosphated using the procedure from Dumesic *et al*.[1] Briefly, the catalysts were prepared by stirring 10 g of support material (niobic acid hydrate or titanium dioxide) in 1 M phosphoric acid solution for 48 h. The catalyst materials were then separated from aqueous solution by centrifugation at 10,000 rpm for 5 min and subsequently washed with deionized water three times. Next, the solid powders were dried at 120 °C for 12 h (10 °C min^{-1} ramp) and calcined at 400°C (5 °C min^{-1} ramp) for 5 h followed by grinding and sieving to +80 mesh particles sizes.

Palladium nanocrystals were deposited onto the acidic supports using a typical incipient wetness procedure.[2] For preparing 5 wt% Pd relative to support, 625 mg of palladium nitrate dihydrate was dissolved in 3 mL of water and mixed with 4.75 g of metal oxide support with stirring and sonication. Next, the catalyst slurries were dried under air at 107 °C for 6 h (10 °C min^{-1} ramp) and 265 °C for 2 h (5 °C min^{-1} ramp) followed by grinding and sieving of the catalysts to +80 mesh particle sizes. Finally, the precursor crystals were reduced to Pd in a tube furnace by first purging under 200 cm^3 (STP) min^{-1} of N_2 for 1 h before reduction at 265 °C (5 °C min^{-1} ramp) for 5 h under 200 cm^3 (STP) min^{-1} of H_2.

Simulated regeneration of $Pd/NbOPO_4$ was performed by loading 1 g of as-synthesized catalyst into a tube furnace, heating to 350 °C under N_2 (2 °C min^{-1} ramp), holding for 2 h under zero air, cooling down to 35 °C under N_2, heating to 265 °C under N_2 (2 °C min^{-1} ramp), holding for 3 h under H_2, and cooling to room temperature under N_2. The reduction-oxidation cycle was repeated three more times for the Regen 4x sample. All steps were under 200 cm^3 (STP) min^{-1} of gas flow.

Nitrogen physisorption was performed using a Quadrasorb evo (Quantachrome) to assess catalyst morphology. In a typical measurement, 0.10 g of catalyst was degassed under vacuum at 200 °C for 16 h directly before analysis. Full adsorption and desorption isotherms were recorded for each sample at -196 °C. Surface area was computed using the BET method, while pore volume and pore size distribution were determined using the BJH method for the desorption isotherm branch.[3]

Pyridine adsorption diffuse reflectance Fourier transform infrared spectroscopy (Pyr-DRIFTS) measurements were performed using a Thermo Nicolet iS50 FT-IR spectrometer equipped with a Harrick Praying Mantis reaction chamber. Metal oxide samples were treated at 350 °C (5 °C min^{-1} ramp) for 2 h under flowing Ar, cooled to 150 °C and purged for Ar for 10 min before collecting a background spectrum. The samples were then dosed with pyridine vapor by flowing Ar through a pyridine-filled bubbler at room temperature for 5 min before removing physisorbed pyridine under Ar by heating to 200 °C (5 °C min^{-1} ramp) and holding for 30 min. The samples were cooled back to 150 °C and the spectra were collected by taking 64 scans at a resolution of 4 cm^{-1}. The background spectra were subtracted from the average spectra before determining the relative ratio of Brønsted and Lewis acid sites by the peak area of the vibrational modes near 1445 cm^{-1} (Lewis) and 1540 cm^{-1} (Brønsted).

Pd dispersion was measured by pulsed CO chemisorption using an Autochem II 2920 (Micromeritics). Approximately 0.10 g of catalyst was loaded into a quartz u-tube and supported by quartz wool. After purging the system with helium, the catalyst was pretreated in helium at 200 °C for 1 h and reduced in a premixed stream of 10% hydrogen (balance argon) for 2 h at 150 °C. After purging with helium for 30 min at 150 °C and then cooling to 40 °C, 15 sequential pulses of premixed 10% CO (balance helium) were injected into helium carrier gas flowing through the catalyst bed at 50 cm^3 (STP) min^{-1}. The calibrated volume of the injection loop was used to calculate the quantity of CO adsorbed, and the Pd dispersion was then estimated assuming a 1:2 binding of CO to Pd and bulk Pd content of 5% by weight.

Temperature programmed desorption of ammonia was performed using an Autochem II 2920 (Micromeritics) to measure catalyst acidity. Approximately 0.10 g of catalyst was loaded into a quartz u-tube and supported by quartz wool. After purging the system with helium, the catalyst was pretreated by ramping to 120 °C for 1 h, then 500 °C for 2 h in flowing helium. After cooling to 120 °C, a stream of premixed 10% NH_3 (balance helium) was passed over the catalyst for 1 h to saturate acidic sites on the catalyst surface. Following a 2-h helium purge at 120 °C to remove physisorbed NH_3, the sample temperature was ramped to 500 °C at 10 °C min^{-1} in helium carrier gas at 50 cm^3 (STP) min^{-1}, while NH_3 concentration in the effluent was monitored by a thermal conductivity detector (TCD). After calibrating the TCD, the desorption peak area was used to calculate the total quantity of acid sites by assuming a 1:1 stoichiometry of NH_3 binding to acid sites.

X-ray diffraction (XRD) spectra were collected using a Rigaku Ultima IV diffractometer equipped with a Cu Kα X-ray source and a dTex high speed detector. Powdered catalyst samples were analyzed with the source set at 44 kV and 40 mA over a range of 20-80° two-theta with a scan rate of 5° min^{-1} and a data spacing of 0.02°.

Phosphorus content was measured in the liquid effluent from a continuous flow test with $Pd/NbOPO_4$ catalyst after 33 h of reaction time. The sample was analyzed according to ASTM D3231 standard test for phosphorus content in gasoline by the Southwest Research Institute.

Pd leaching was analyzed via inductively coupled plasma-optical emission spectroscopy (ICP-OES) (Agilent 5110). Initially, approximately 5 g of the reaction effluent was weighed into a Teflon vessel and completely evaporated under nitrogen flow. The organic film remaining at the bottom of the vessel was dissolved in 2 mL of aqua regia (3:1 HNO_3:HCl). This mixture was heated in a Teflon vessel at 210 °C for 45 min in a microwave digestion system (CEM MARS5) operating at 800 W. The digestate was then diluted to 10 mL with DI water and analyzed. Calibration standards for Pd were made at 0.01, 0.1, 1, 5, and 10 ppm in the same dilute aqua regia matrix. Elemental concentrations were quantified using the 340.458 nm emission peak for Pd. Results were reported as ppb on a sample basis (μg Pd kg^{-1} of unevaporated product mixture).

Thermogravimetric Analysis-Fourier Transform Infrared spectroscopy (TGA-FTIR) experiments were performed in a Setaram Setsys Evolution TGA coupled, via a heated transfer line at 200 °C, with a Nicolet 6700 FTIR with a gas cell maintained at 225 °C to prevent vapor condensation. The gas flow rate used in the experiments was 50 cm^3 (STP) min^{-1}. The samples (~ 100 mg) were placed inside a crucible with one closed end and, under a flow of nitrogen, the samples were held at 20 °C for 10 min to ensure the furnace and gas lines were sufficiently purged of other gases, then the gas atmosphere was switched to dry air and the temperature was ramped to 200 °C at a rate of 20 °C min^{-1} and held at 200 °C for 20 min and subsequently ramped to 550 °C at a rate of 20 °C min^{-1} and held at 550 °C for 30 min

Scanning transmission electron microscopy (STEM) imaging and energy dispersive x-ray spectroscopy (EDS) elemental mapping were performed on a FEI Talos F200X TEM at 200 kV equipped with a high-angle annular dark field (HAADF) detector and four Bruker XFlash 120 mm^2 silicon-drift detectors. Alternately, imaging was performed on an aberration-corrected JEOL 2200FS STEM, equipped with a CEOS GmbH corrector on the probe-forming lenses and operated at 200kV with simultaneous BF- and HAADF-STEM imaging and equipped with Bruker XFlash® 6T/30 silicon drift detector XFlash® 6T/30 for EDS analysis. High resolution STEM imaging was performed on an aberration-corrected JEM-ARM200F NEOARM, operating at 200kV.

Catalytic testing

Pre-screening of catalysts and reactants were performed with a multi-batch reactor system (Parr Instrument Co). Feed solution (20 mL, equimolar alcohol & ketone) and catalyst (681 mg of single-phase catalyst or metal oxide support, 231 mg of 5 wt% Palladium on activated carbon from Sigma Aldrich when applicable) were added to 75-mL reactor cups. The vessels were massed, sealed, purged three times first with He, then purged with H_2 and pressurized to 1000 psig of H_2 before heating to the desired temperature over a period of about 30 min. The mixture was stirred at 800 rpm throughout the 1 h reaction time before

quenching in an ice batch to terminate the reaction. The product solution was filtered through 0.2-μm nylon membranes to separate the solid catalyst and analyzed by GC/MS and GC/Polyarc-FID.

A custom-built trickle bed flow reactor was utilized for continuous flow reductive etherification reactions and a simplified flow diagram is shown in **Figure S1**. The reactor was equipped with two mass flow controllers calibrated for argon and hydrogen gas (Brooks Instruments), a back-pressure regulator calibrated for argon (Brooks Instruments), an HPLC pump for high-pressure liquid injection (Chromtech), a clamshell furnace (Carbolite Gero) surrounding a 0.5" Dursan-coated stainless steel tube containing the catalyst bed, heat tracing (Briskheat) on the gas and liquid inlets to pre-heat the reaction mixture before reaching the catalyst bed, and dual thermocouples measuring the temperature along the heated inlet and in the center of the catalyst bed. The reactors were leak-checked with argon before flushing and pressurizing with hydrogen for each test. The catalyst (0.5 or 2.1 g) was held in place with a packing of glass beads, 30-50 mesh sand, and a glass wool plug at the outlet. After passing through the reactor, the effluent was cooled with a tube-in-tube heat exchanger held at 2 °C and collected in a 100 mL knockout pot (Parr) with a hand-valve for periodic liquid sampling. The liquid reactant feed of equimolar 4-heptanone and 1-butanol was delivered at flow rates of 0.05-0.15 mL min^{-1} to achieve the desired WHSV of 1.2-4.8 h^{-1}. To reduce initial reactor instability, the catalyst bed was pre-wet before each test with 0.5 mL min^{-1} of liquid flow and 150 cm^3 (STP) min^{-1} at room temperature for 30 min. Liquid effluent samples were collected from the knockout pot periodically and analyzed by GC/MS and GC/Polyarc-FID.

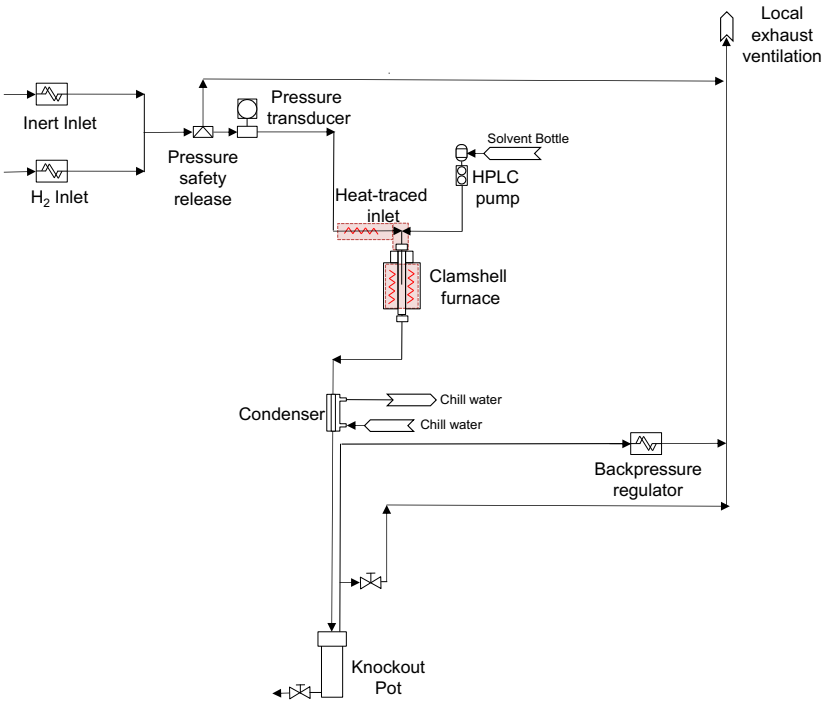

Figure S1. Simplified flow diagram for the custom-built trickle bed flow reactor used for continuous flow reaction testing.

Conversion of ketone reactants is reported as the molar change in the ketone reactant concentration divided by the initial moles of ketone reactant, as insignificant carbon is lost to the gas phase.

$$Conversion = \frac{Mol_{ketone,in} - Mol_{ketone,out}}{Mol_{ketone,in}} \quad (1)$$

For **Figure 1 (b)**, conversion results are reported for ketone, as indicated, with carbon balance and mass yield results provided in **Table S1, S4, S5, and S6.** Mass yield was calculated from GC/Polyarc-FID integrations based on methane response (see method below), with nonane as an internal standard to quantify the carbon balance of liquid products.

$$Yield\ (mass\ \%) = \frac{Mass_{product,out}}{\left(Mass_{ketone,in} + Mass_{alcohol,in}\right)} * 100\% \quad (\mathbf{2})$$

Selectivity data for target ether products is defined by the molar yield of the reductive etherification product divided by the molar yield of all products measured by GC/MS (target ether, non-target alcohol, non-target ether, or non-target hydrocarbons).

$$Selectivity\ (\%) = \frac{Yield_{Target\ Ether}}{\left(Yield_{Target\ Ether} + Yield_{Non-target\ alcohol} + Yield_{Non-target\ ether} + Yield_{non-target\ hydrocarbon}\right)} * 100\% \ (\mathbf{3})$$

Liquid product mixtures obtained from reductive etherification were analyzed via an Agilent 7890 GC system with a Polyarc equipped with a combination flame ionization detector and mass spectrometer (FID-MS) detection for confirmation of compound identity and estimation of compound concentration and purity. The Polyarc (Activated Research Company) is a catalytic system which converts organic compounds to methane before analysis with traditional FID to eliminate the need for calibration of FID response for each compound. This allows quantitation of chromatographically separated compounds by comparison of FID area response for most compounds irrespective of compound class. Calculation of compound concentration in the sample with the Polyarc-FID system is based on the following equation:

$$Carbon_{sample} = \frac{Area_{sample} * Carbon_{standard}}{Area_{standard}} \quad (\mathbf{4})$$

The GC system incorporated a split plate which allowed simultaneous analysis of a separate portion of the GC column eluent by MS detection (i.e., not processed through the Polyarc). GC analysis utilized an HP-5MS column (30 m x 0.25 4 mm), split injection (25:1), injection volume of 1 µL, inlet temperature of 260 °C, oven temperature programming (40 °C for 2 min, then 18 °C min^{-1} to 280 °C for 0 minutes), and helium carrier gas (constant flow mode, 29 cm sec^{-1}). Samples were typically prepared by adding 4 µL of sample to 1.0 mL of solvent (usually acetone) plus 2 µL of nonane as the internal standard.

Technoeconomic analysis

In order to evaluate the economic impacts of various process variables, a techno-economic process model was developed. This model utilized Aspen Plus to model a facility which would convert wastewater sludge into butyric acid via anaerobic digestion. The butyric acid would then be catalytically upgraded to 4-butoxyheptane, a potential diesel bioblendstock. The facility would be co-located with an existing wastewater treatment facility and process 300 dry tonnes per day (TPD) of wastewater sludge. A simplified block flow diagram of the process is shown in **Figure S8**.

Wastewater sludge, modeled as having the composition shown in **Table S6**, is fed into an anaerobic basin. The 17.5 MM gallon basin, with a hydraulic retention time of 22 days and a volatile solids loading factor of 4.2 kg/day/m^3, facilitates the digestion of the accessible portion of the sludge (carbohydrates, lipids, and proteins) to butyric acid according to the reactions shown in **Table S7**. The carbon balance on these stoichiometric equations has been validated by metabolic pathways; however, note that the reactions are balanced with H_2, which is not observed experimentally. To rectify this, H_2 is separated from the product stream and is not utilized further in the process. Any H_2 required by downstream operations is therefore purchased. Reaction conversions are manipulated so that the chemical oxygen demand (COD) of the solids is reduced by 55%. Though research on COD reduction in this specific application (anaerobic digestion of wastewater sludge to volatile fatty acids) is limited, this is seen as a conservative estimate as compared to general anaerobic digestion of similar feedstocks.[4, 5]

A pump-around loop from the basin goes to a pertractive membrane system where an organic solvent (trioctylphosphine oxide, TOPO) selectively removes butyric acid across the membrane; a recovery system adapted from recent studies on the biochemical conversion of lignocellulosic biomass.[6] A simplified process flow diagram is shown below in **Figure S9**. It should be noted that although this technology has shown promising results for similar applications (i.e. recovery of butyric acid from fermentation of lignocellulosic biomass), additional research advancements would have to be made for industrial application. From the aqueous side of the pump-around loop, a slip stream is sent to the co-located wastewater treatment plant for treatment of the digestate. Following butyric acid recovery, the organic solvent/acid mixture is sent to a solvent recovery column, with the bottom stream containing nearly pure TOPO solvent, which is recycled, and the top stream containing nearly pure butyric acid.

The butyric acid is then split into two parallel reaction streams. Key process parameters for the butyric acid to C11 ether portion of the process are outlined in **Table S8** and a simplified process flow diagram of the reaction section is shown in **Figure S10A**. The first reactor runs a gas phase ketonization reaction at 365°C and atmospheric conditions over a ZrO_2 catalyst to produce 4-heptanone, as described in previous work by Davis *et al*.[6] The CO_2 produced is separated via flash and a scrubber is used to recover the 4-heptanone. Water is separated from the 4-heptanone using a decanter. The second reactor runs a C4 acid reduction reaction to n-butanol in the vapor phase using hydrogen at high pressure (25 atm) over a RuSn-ZnO catalyst.[7] The hydrogen is purchased at a price of $1.46/ton and compressed via a multistage compressor.

Next, the butanol and 4-heptanone undergo a liquid phase etherification reaction at 190°C and 1000 psi in the presence of hydrogen (also purchased and compressed) over a $Pd/NbOPO_4$ catalyst to produce 4-butoxyheptane. In addition to the desired reaction to 4-butoxyheptane, multiple side reactions are modeled. A full list of reactions can be found in **Table S9**. The process flow representation for the separations section is shown in **Figure S10B**. The effluent of the etherification reactor is sent to the product column, which separates out 4-butoxyheptane out of the bottom, with all other components exiting in the distillate stream. This stream is sent to a decanter, yielding an organic phase, which is sent downstream for further separations, and a water stream, sent to the wastewater treatment facility.

The organic stream from the decanter is first sent to a molecular sieve dryer to remove the majority of the residual water, due to the presence of a ternary azeotrope between water, butanol, and heptane. The effluent from the dryer is sent to a vacuum distillation column meant to separate out heptane. The distillate from this column is made up of an azeotropic mixture of heptane and butanol. This stream is then sent to a pressurized (30 psia) column which shifts the azeotrope and allows for a pure heptane bottoms product, which serves as a gasoline-range blendstock. The distillate of this column is recycled back to the vacuum column.

The bottom of the vacuum column is sent to a series of distillation columns. The first column separates butanol for recycling, while the second column separates 4-heptanol for inclusion in the product blendstock. Finally, we are left with a mixture of 4-heptanone and DBE. This separation proves very difficult due to an azeotrope forming at about 0.4 mass fraction of DBE which does not change significantly with pressure. The stream is sent to a column which gives a pure 4-heptanone bottoms stream for recycling and a distillate stream close to the azeotrope composition. Although this distillate stream is responsible for a sizeable yield loss in the overall scheme, further separation was determined to be not economically viable at this time and it is sent to be combusted in the steam boiler.

The biofuel facility includes a natural gas boiler for high- and low-pressure stream and a separate hot oil system for high temperature applications which also utilizes natural gas. A cooling water system is also utilized to meet facility cooling demands.

Economic Analysis Approach

Aspen Plus process models were developed based on the conceptual process designs described above. The material and energy flows in the process and the overall variable and fixed operating costs, as well as the capital costs, were then estimated for the integrated design and the calculated flow rates. The capital costs, which are outlined for Case 1 in **Table S10**, are based on vendor designs when available. The details of these equipment designs have been published by Davis *et al*.,[6] Dutta *et al*,[8] and Humbird *et al*.[9] Variable and fixed operating costs for Case 1 are supplied in **Tables S11** and **S12**, respectively. The cost of the $Pd/NbOPO_4$ catalyst was estimated using the CatCost model[10] and the Step Method developed by Baddour *et al.*[11] with the palladium precursor price based upon a palladium cost of $12,539/kg (2018 dollars) and the $NbOPO_4$ support cost at $44/kg (per CBMM).

To estimate the minimum selling price of the bioblendstock, a discounted cash flow analysis was applied under a specific set of financial assumptions. These financial assumptions are reviewed in **Table S13**, which are based on a mature *n-th* plant and consistent with prior published work.[6, 8, 9] Finally, a cost breakdown of the TEA model by area is shown in **Figure S11** for Case 1.

Section S2: Experimental Results (in order of mention in main text)

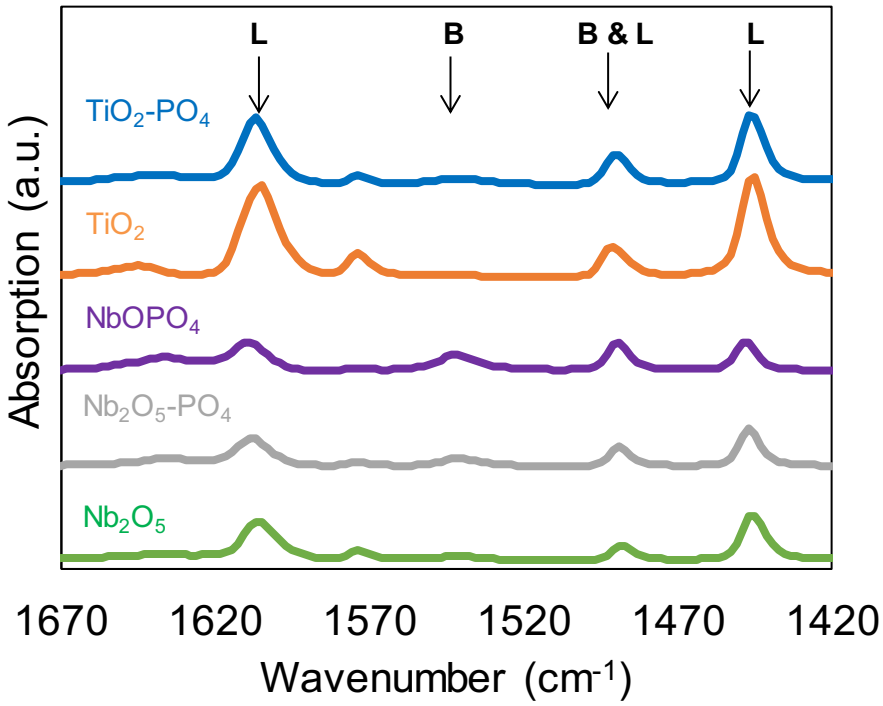

Figure S2. Pyridine-DRIFTS spectra for all acidic supports tested in this paper with relevant peaks corresponding to Brønsted (B) (at 1542 cm^{-1}) and Lewis (L) (at 1608 and 1446 cm^{-1}) and total (1491 cm^{-1}) acid sites denoted in the figure inset.

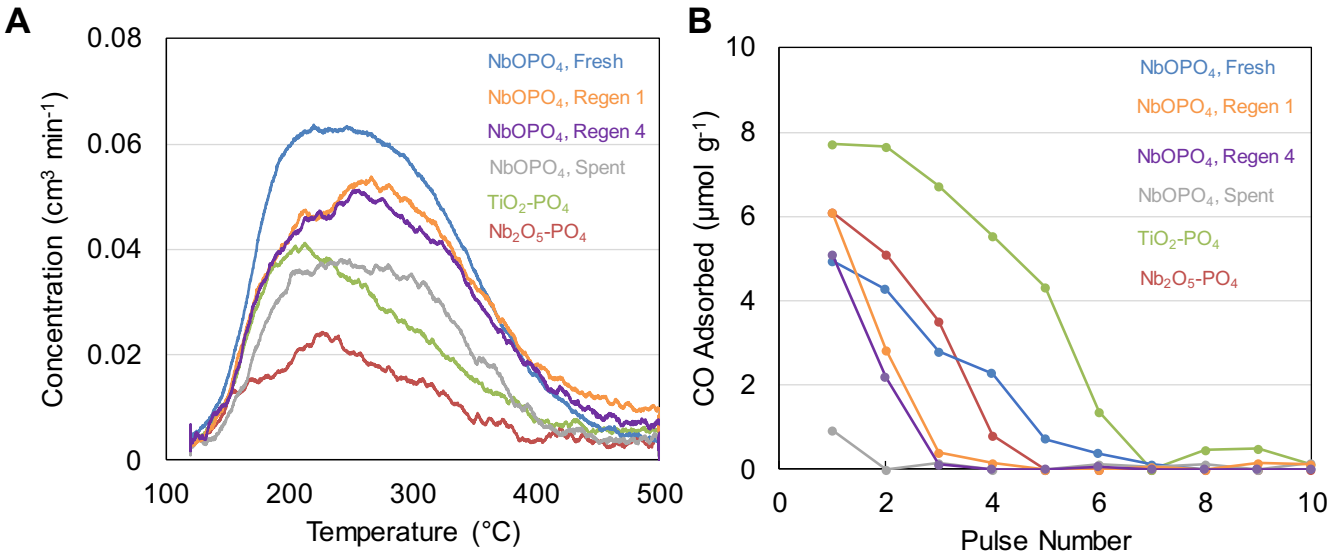

Figure S3. Raw chemisorption data from NH_3 temperature programmed desorption (a) and CO pulse chemisorption (b).

Table S1. Liquid-phase carbon balance for batch reductive etherification tests over various solid acid catalysts shown in Figure 1. Reaction conditions were as follows: 9.9 g of 4-heptanone, 6.4 g of 1-butanol (1:1 molar), 230 mg Pd/C (when applicable) and 680 mg solid acid or single-phase catalyst, 190 °C, initial 1000 psig H_2, 1 h, stirred at 800 rpm in 75-mL batch reactor.

Catalyst	4-Heptanone (wt %)	1-Butanol (wt %)	4-BH (wt %)	4-Heptanol (wt %)	n-Butyl Ether (wt %)	n-Heptane (wt %)
Pd/C & TiO_2	44.2 ± 1.7	29.3 ± 3.0	21.2 ± 4.1	5.3 ± 0.6	0	0
Pd/C & TiO_2-PO_4	46.0 ± 1.0	20.1 ± 0.3	28.4 ± 0.8	4.6 ± 0.4	0.7 ± 0.2	0.2 ± 0.0
Pd/TiO_2-PO_4	50.3 ± 0.8	22.6 ± 0.2	19.4 ± 0.6	7.6 ± 0.2	0.5 ± 0.5	0.3 ± 0.1
Pd/C & Nb_2O_5	47.5 ± 0.7	26.6 ± 0.5	20.8 ± 0.3	4.9 ± 0.1	0.2 ± 0.2	0
Pd/C & Nb_2O_5-PO_4	25.6 ± 1.0	19.1 ± 0.1	43.5 ± 0.7	10.3 ± 0.5	0.5 ± 0.1	0.8 ± 0.1
Pd/Nb_2O_5-PO_4	31.5 ± 0.5	15.1 ± 0.4	42.2 ± 0.4	9.0 ± 0.1	0.9 ± 0.1	0.8 ± 0.1
Pd/C & $NbOPO_4$	11.6 ± 1.8	18.0 ± 1.2	54.8 ± 0.9	10.0 ± 0.6	0.8 ± 0.2	4.8 ± 0.0
Pd/$NbOPO_4$	13.8 ± 0.4	9.5 ± 0.5	62.7 ± 0.6	10.3 ± 0.2	1.3 ± 0.1	2.9 ± 0.2

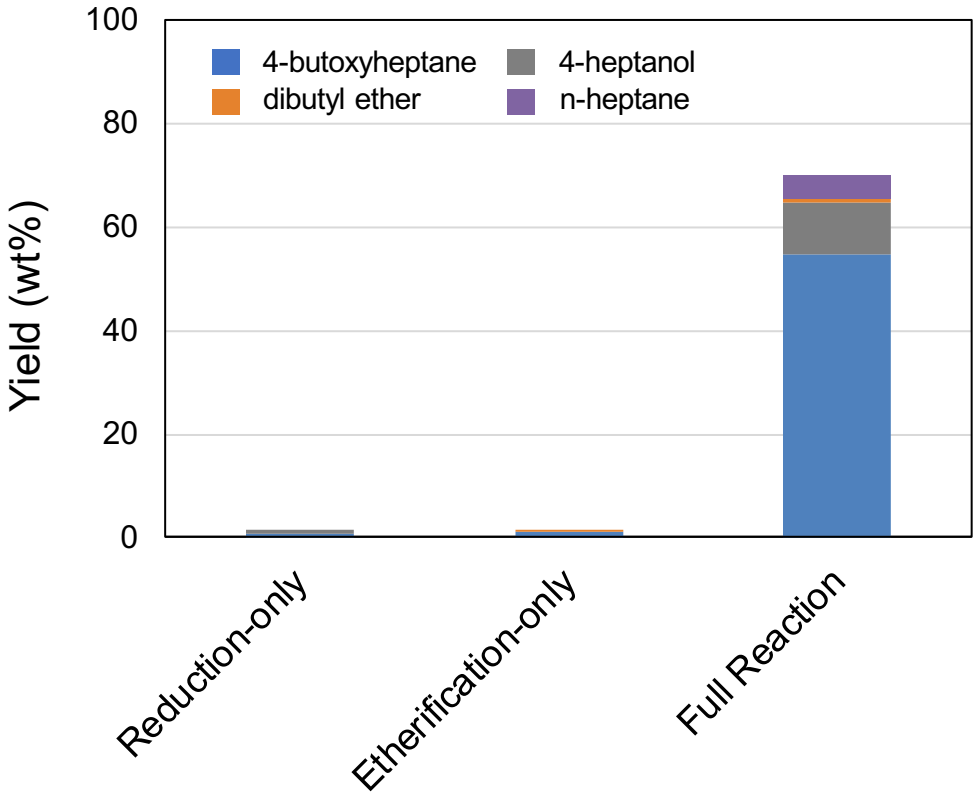

Figure S4. Batch reactor screening tests evaluating the reaction pathway shown in Scheme 2. Conditions: 190 °C, initial 1000 psig H_2, 800 rpm stirring, 230 mg Pd/Carbon, 680 mg $NbOPO_4$, 20 mL equimolar 4-heptanone and n-butanol, 1 h reaction time. Reduction-only: Pd/Carbon catalyst alone, no $NbOPO_4$ acid catalyst. Etherification-only: 4-heptanol starting material in place of 4-heptanone. Full reaction: exact conditions outlined above for comparison (also shown in Figure 1a).

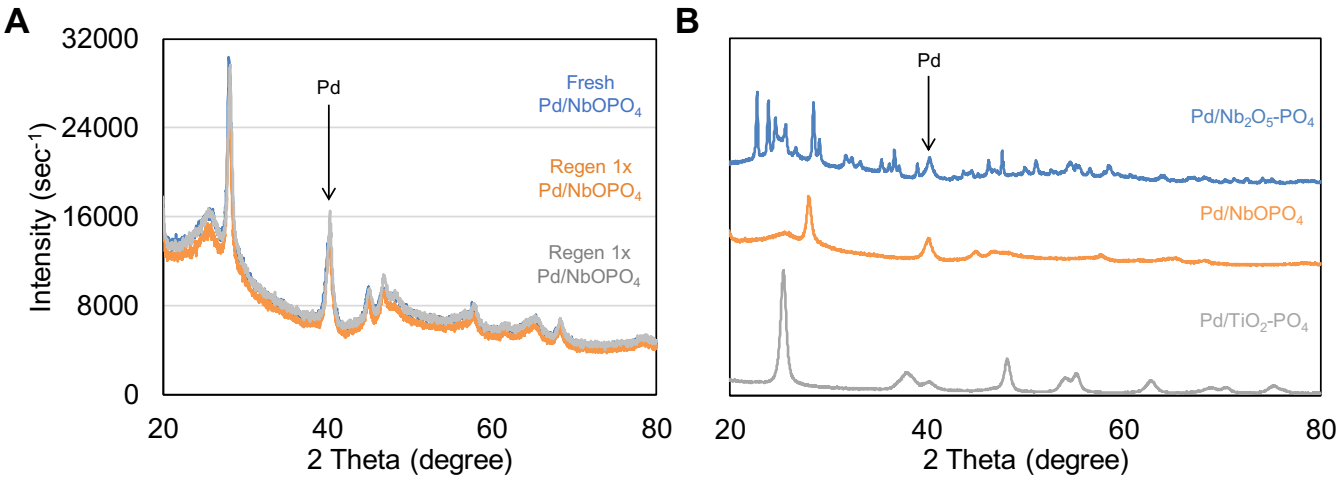

Figure S5. X-ray diffraction scattering spectra for single-phase catalysts including fresh $Pd/NbOPO_4$ sample, 1-cycle simulated regeneration, and 4-cycle simulated regeneration (a) and a comparison of three single-phase catalysts as-synthesized (b). Relevant peaks include the Pd peak used for crystal size determination at 40.2 degrees.

Table S2. Palladium nanoparticle (Pd NP) size distributions from STEM imaging used to prepare histogram graphs in Figure 2.

Histogram Bins (Pd NP size ranges, nm)	Fresh $Pd/NbOPO_4$	117 h Spent $Pd/NbOPO_4$	Regen 4x $Pd/NbOPO_4$
0-2	10	0	278
2-4	12	21	93
4-6	28	36	17
6-8	26	30	21
8-10	37	27	33
10-12	19	14	26
12-14	12	11	14
14-16	8	5	13
16-18	2	7	15
>18	9	12	17

Table S3. Liquid-phase carbon balance for batch reductive etherification tests with various substrates shown in Figure 3b. Reaction conditions were as follows: 20 mL of equimolar alcohol and ketone reactants, 0.68 g $Pd/NbOPO_4$ catalyst, 190 °C, initial 1000 psig H_2, 1 h, stirred at 800 rpm in 75-mL batch reactor. The asterisk for the 1-isopropoxybutane reaction denotes a liquid side-products that were not detected through GC/MS.

Target Product	Reactant Ketone (%)	Reactant Alcohol (%)	Target Ether (%)	Non-target Alcohol (%)	Non-target Ether (%)	Non-target Hydrocarbon (%)
1-isopropoxybutane	12.2 ± 0.6	26.7 ± 0.8	39.5 ± 0.3	0	0.9 ± 0.1	33.6 ± 0.4*
4-hexoxyheptane	20.4 ± 0.7	14.2 ± 0.2	56.3 ± 0.9	6.4 ± 0.1	1.4 ± 0.5	1.2 ± 0.1
6-ethoxyundecane	47.4 ± 1.1	5.3 ± 0.1	43.4 ± 1.8	0	0	1.2 ± 0.1
4-octoxyheptane	7.9 ± 0.6	14.9 ± 0.7	70.0 ± 0.5	5.0 ± 0.3	0	2.7 ± 0.3
4-ethoxyheptane	38.0 ± 3.5	10.2 ± 1.5	41.1 ± 2.8	8.0 ± 1.6	0	1.9 ± 0.5

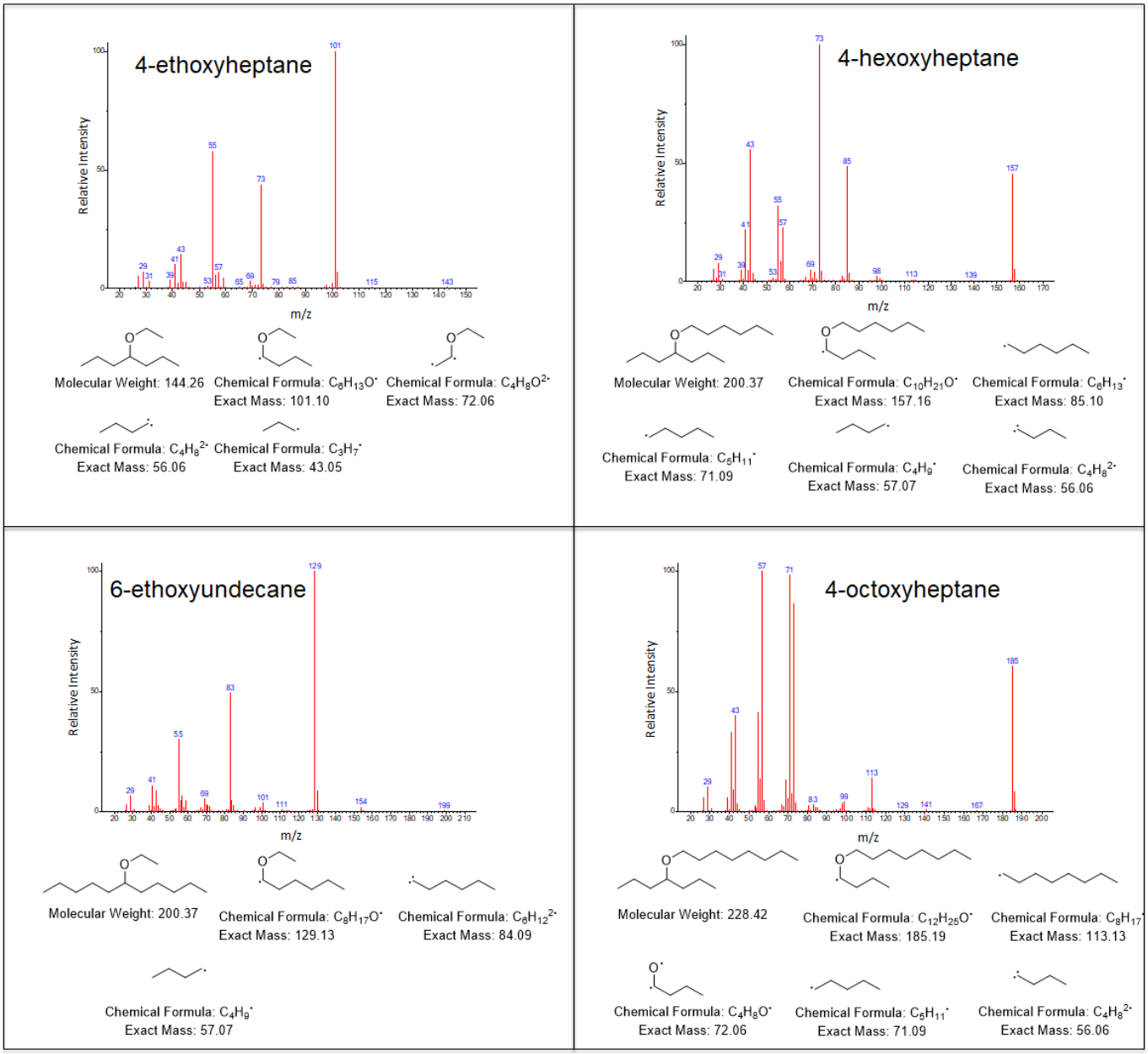

Figure S6. Mass spectral fragment patterns and predicted fragment masses for ether molecules absent from the NIST mass spectral database (2011) identified with gas chromatography.

Table S4. Mass yields for continuous reductive etherification tests over various solid acid catalysts in a trickle bed reactor shown in Table 2 and Figure 4. Reaction conditions were as follows: 4-heptanone and 1-butanol (1:1 molar) liquid feed at 0.05 mL/min, ½" outer diameter reactor tube packed with 0.5 g catalyst bed ($Pd/NbOPO_4$ unless noted), H_2 flow 30 sccm at 1000 psig, bed temperature of 190 °C unless noted. Duplicate reactions were performed with $Pd/NbOPO_4$ at five temperatures with average values reported and error bars indicating standard deviation.

Condition	4-Heptanone (wt %)	1-Butanol (wt %)	4-BH (wt %)	4-Heptanol (wt %)	n-Butyl Ether (wt %)	n-Heptane (wt %)
Pd-TiO_2-PO_4	42	18	17	6	1	0
Pd-Nb_2O_5-PO_4	40	17	16	7	1	1
Pd-$NbOPO_4$	38 ± 2	16 ± 1	29 ± 3	4 ± 1	1 ± 0	2 ± 1
125 C	31 ± 1	14 ± 0	38 ± 3	5 ± 1	3 ± 0	7 ± 0
150 C	49 ± 1	20 ± 1	21 ± 2	3 ± 0	1 ± 0	0
175 C	54 ± 0	21 ± 0	14 ± 2	2 ± 1	1 ± 0	1 ± 0
200 C	58 ± 1	23 ± 1	5 ± 1	1 ± 0	1 ± 0	0
Spent (117 h time-point)	46	18	20	2	1	0
Regen 1x	23	13	41	4	3	9
Regen 4x	24	13	40	4	3	9

Table S5. Mass yields for continuous reductive etherification tests at various gas and liquid flow rates in a trickle bed reactor shown in and Figure 4c. Reaction conditions were as follows: 4-heptanone and 1-butanol (1:1 molar) liquid feed, ½" outer diameter reactor tube packed with 2.1 g catalyst bed ($Pd/NbOPO_4$ unless noted), varied H_2 flow at 1000 psig, bed temperature of 190 °C except for Condition Pd/C & A-15 which was performed at the maximum allowable temperature of 120 °C. A duplicate reaction was performed at Condition 2 with average values reported and error bars indicating standard deviation.

Case	H_2 Equiv	H_2 Flow (sccm)	WHSV (sec^{-1})	Liquid (mL/min)	4-Heptanone (wt %)	1-Butanol (wt %)	4-BH (wt %)	4-Heptanol (wt %)	n-Butyl Ether (wt %)	n-Heptane (wt %)
1	1.9	8	1.2	0.05	17	10	46	8	5	10
2	3.8	16	1.2	0.05	11 ± 6	9 ± 0	53 ± 1	8 ± 2	4 ± 0	10 ± 4
3	5.6	25	1.2	0.05	10	7	58	8	4	9
4	1.9	32	2.3	0.10	30	14	42	6	2	3
5	1.9	48	3.5	0.15	33	13	39	6	2	2
*Pd/C A-15**	1.9	48	3.5	0.15	15	13	46	18	1	2

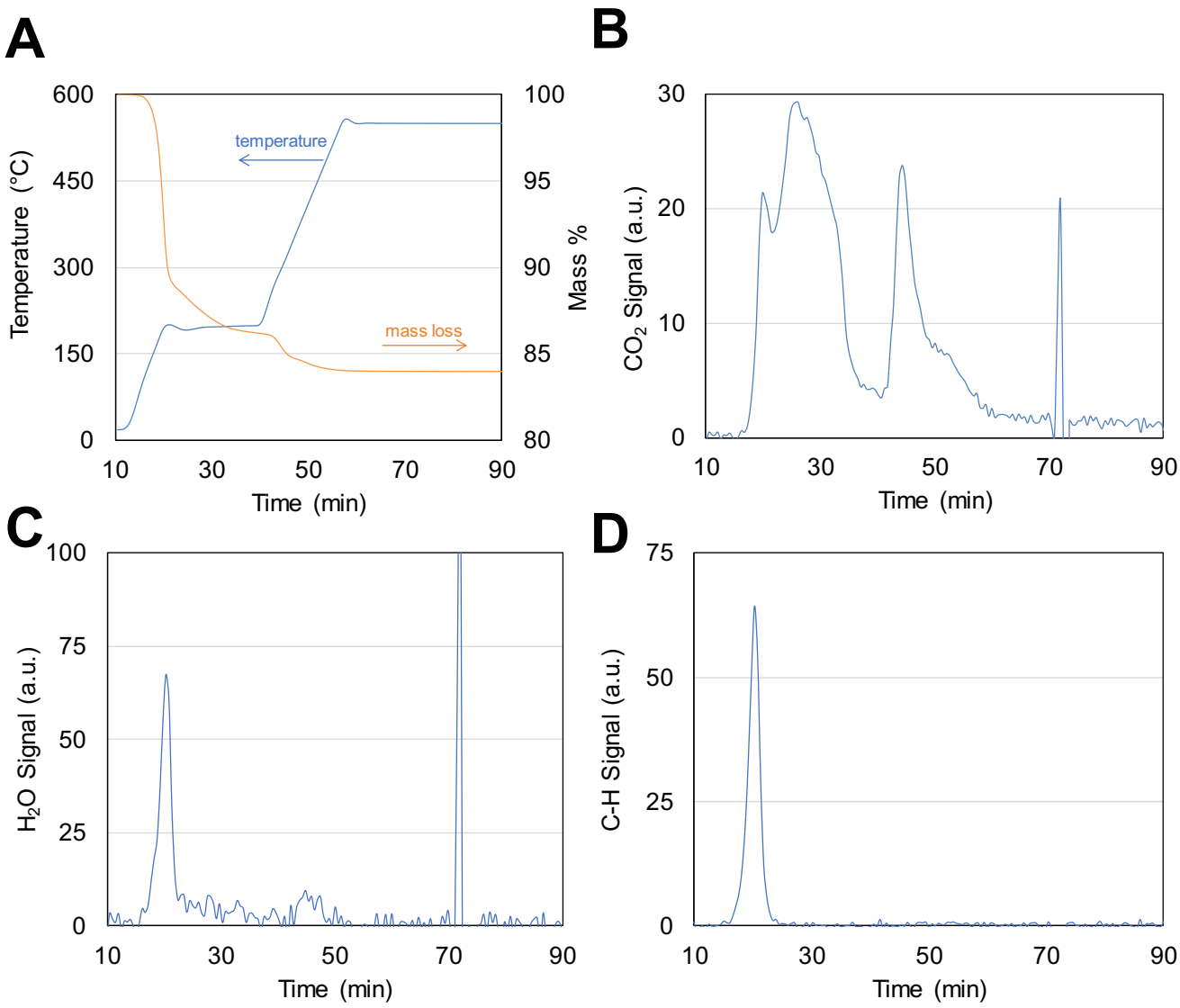

Figure S7. Raw thermogravimetric analysis data of temperature and weight loss (mass %) during time for the 117-h spent Pd/$NbOPO_4$ catalyst including FTIR signal values for carbon dioxide (b) water (c) and C-H stretching (d).

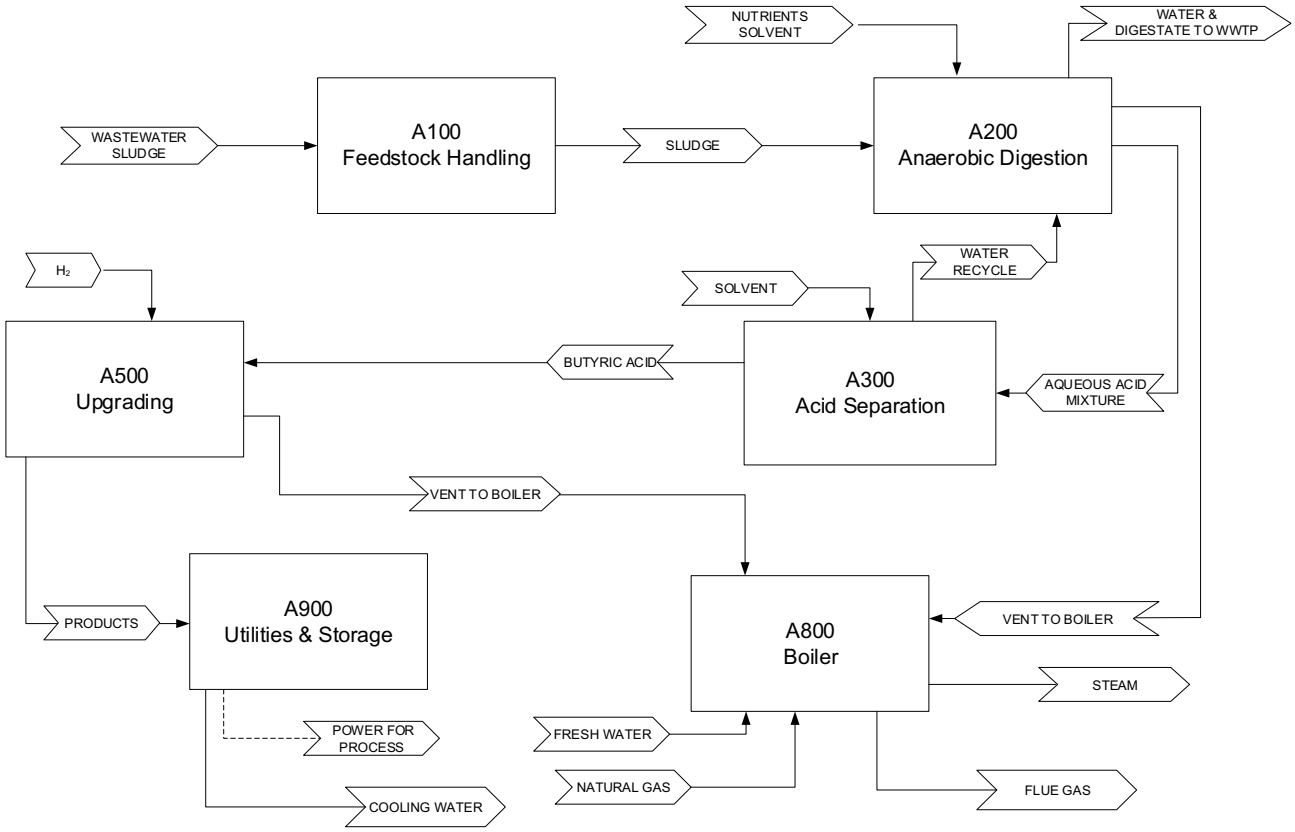

Figure S8. Block flow diagram showing key process areas of the techno-economic model.

Table S6. Modeled feed composition of the wastewater sludge for the techno-economic model.

Component	Wt %
Cellulose (modeled as glucan)	16
Lipids (modeled as triolein, $C_{57}H_{104}O_6$)	24
Protein (modeled as $CH_{1.57}O_{0.31}N_{0.29}S_{0.007}$)	18
Indigestible Matter	42

Table S7. Modeled reactions for anaerobic digestion. Reaction conversions are set to reach a 55% COD reduction, not including acid and H_2 produced. "Cell Mass" is represented by $C_5H_7O_2N$.

Reaction	Stoichiometry
1	Cellulose + H_2O ⟶ Butyric Acid + 2 CO_2 + 2 H_2
2	Lipid + 42 H_2O + 1.5 NH_3 ⟶ 9 Butyric Acid + 13.5 CO_2 + 1.5 Cell Mass+ 55 H_2
3	Protein + 0.55 H_2O ⟶ 0.11 Butyric Acid + 0.26 CO_2 + 0.06 Cell Mass + 0.01 H_2S + 0.23 NH_3 + 0.33 H_2

Table S8. Summary of key process parameters in the catalytic upgrading portion of the techno-economic model.

Design Basis	
Butyric Acid Reduction	
Temperature	265°C
Pressure	24.67 atm
Catalyst	RuSn-ZnO
WHSV:	0.9 h^{-1}
Ketonization	
Temperature	365°C
Pressure	1 atm
Catalyst	ZrO_2
WHSV	6 h^{-1}
Etherification	
Temperature	190°C
Pressure	1000 psig
Catalyst	$Pd/NbOPO_4$
WHSV	Dependent on case

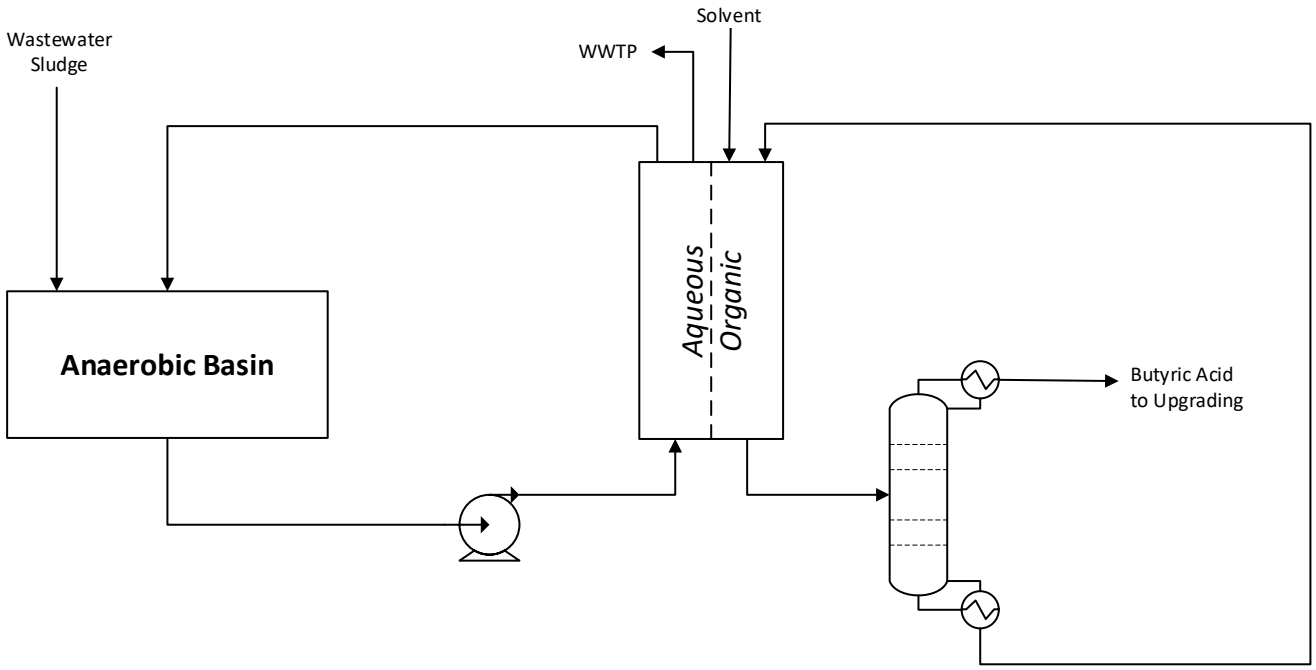

Figure S9. Process flow diagram for the anaerobic digestion and acid separation portions of the techno-economic model.

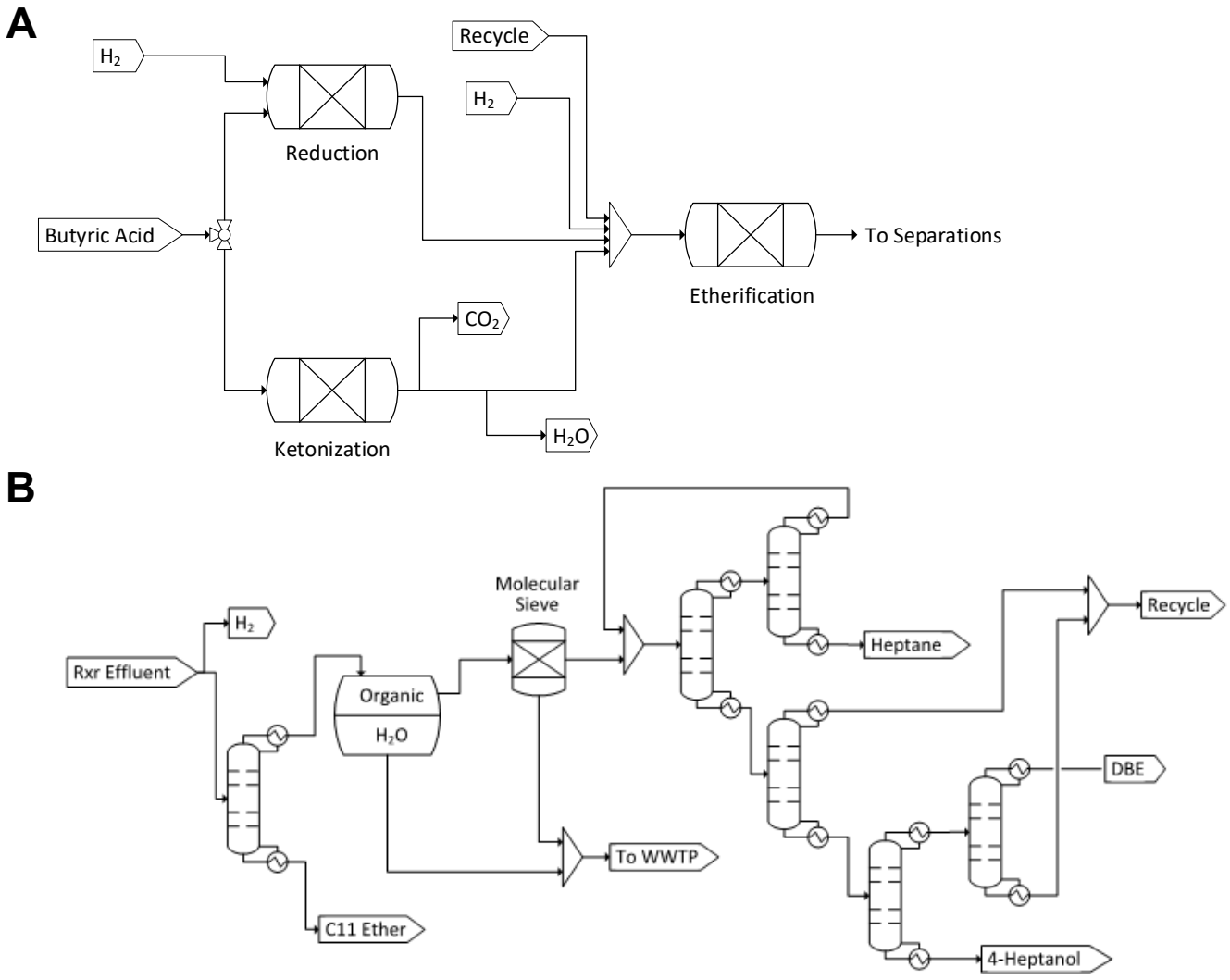

Figure S10. Process flow diagram for the reactive upgrading (A) and separation (B) portions of the techno-economic model.

Table S9. Reaction stoichiometry for 4-butoxyheptane production used in TEA. Conversions are altered between cases to approximately match experimental data.

Reaction	Stoichiometry
Butyric Acid Reduction	Butyric Acid + 2 H_2 → n-Butanol + H_2O
Ketonization	2 Butyric Acid → 4-Heptanone + CO_2 + H_2O
Etherification	n-Butanol + 4-Heptanone + H_2 → 4-Butoxyheptane + H_2O
Etherification side reaction	2 n-Butanol → n-Butyl Ether + H_2O
Etherification side reaction	4-Heptanone + H_2 → 4-Heptanol
Etherification side reaction	4-Heptanol + H_2 → Heptane + H_2O

Table S10. Capital cost breakdown for Case 1 of the techno-economic analysis. Home office and construction fee omitted due to co-location with wastewater treatment facility.

Process Area			Purchased Cost	Installed Cost
A100: Feedstock Handling			$300,685	$300,685
A200: Anaerobic Digestion			$4,995,090	$14,247,681
A300: Acid Separation			$8,193,580	$16,544,985
A500: Upgrading			$7,256,827	$13,856,557
A800: Combined Heat and Power			$534,692	$534,692
A900: Utilities and Storage			$415,475	$786,862
			$21,696,349	**$46,271,462**
Warehouse	4.0%	of ISBL		$1,785,969
Site Development	9.0%	of ISBL		$4,018,430
Additional Piping	4.5%	of ISBL		$2,009,215
Total Direct Costs (TDC)				**$54,085,076**
Prorateable Expenses	10.0%	of TDC		$5,408,508
Field Expenses	10.0%	of TDC		$5,408,508
Project Contingency	10.0%	of TDC		$5,408,508
Other Costs (Start-Up, Permits, etc.)	10.0%	of TDC		$5,408,508
Total Indirect Costs				$5,408,508
Fixed Capital Investment (FCI)				**$75,719,106**
Land				$280,000
Working Capital	5.0%	of FCI		$3,785,955
Total Capital Investment (TCI)				**$79,785,062**

All costs are in 2016 Dollars

Table S11. Variable operating cost breakdown for Case 1 of the techno-economic analysis. Units follow the top labels unless otherwise given.

Feedstock Handling	**kg/hr**	**Cost ($/lb)**	**$MM/yr (2016)**
Feedstock (dry)	12,500	$0.00	$0.00
Anaerobic Digestion			
Corn Steep Liquor	236	$0.034	$0.14
Diammonium Phosphate	34	$0.165	$0.10
Sorbitol	16	$0.330	$0.09
Glucose	72	$0.346	$0.43
Upgrading			
H2 for Reduction	47.6	$0.7306	$0.60
H2 for Etherification	35.1	$0.7306	$0.45
Combined Heat and Power			
Natural Gas (Boiler)	42.1 MMBtu/hr	$5.30/MMBtu	$1.76
Natural Gas (Hot Oil)	3.0 MMBtu/hr	$5.30/MMBtu	$0.58
Ammonia	8.4	0.1900	$0.03
Utilities and Storage			
Cooling Tower Chemicals	0.1	$1.78	$0.00
Makeup Water	10279.5	$0.31/ton	$0.00
Grid Electricity	1,382 kW	$0.0682/kW	$0.74

Table S12. Fixed operating costs for the Case 1 of the techno-economic analysis. Non-operator roles are assumed to be shared with the co-located wastewater treatment facility and are omitted.

		2016 Cost
Total Salaries		$2,740,978
Labor Burden (90% of salaries)		$2,466,880
Other Overhead	**Calculation**	**2016 Cost**
Maintenance	3% of ISBL	$1,339,477
Property Insur. & Tax	0.7% of FCI	$530,034
Total of all fixed costs		$7,077,368

Table S13. Financial assumptions and design basis for TEA.

Financial Assumptions	
Plant life	30 years
Plant throughput	300 dry metric tonnes/day biomass
Cost year dollar	2016$s
Capacity Factor	90%
Discount rate	10%
General plant depreciation	MACR
General plant recovery period	7 years
Steam plant depreciation	MACR
Steam plant recovery period	20 years
Federal tax rate	21%
Financing	40% equity
Loan terms	10-year loan at 8% APR
Construction period	3 years
First 12 months' expenditures	*8%*
Next 12 months' expenditures	*60%*
Last 12 months' expenditures	*32%*
Working capital	5% of fixed capital investment
Start-up time	6 months
Revenues during start-up	*50%*
Variable costs during start-up	*75%*
Fixed costs during start-up	*100%*

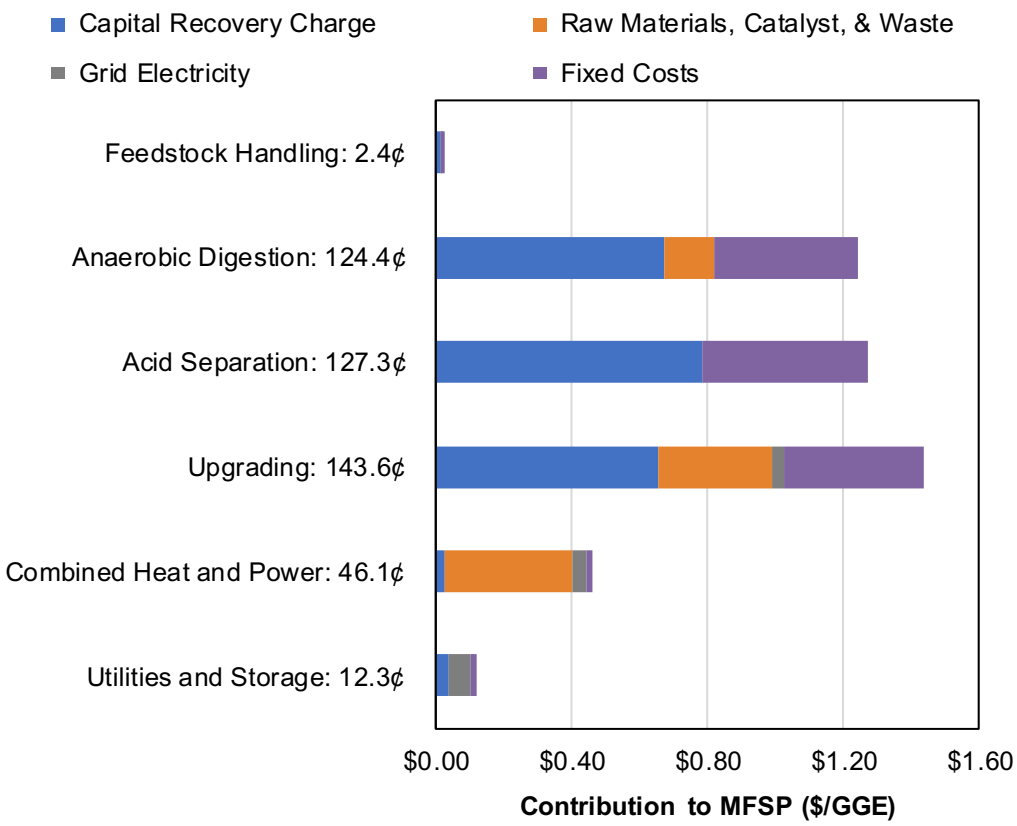

Figure S11. Cost breakdown for Case 1 of the technoeconomic analysis.

Section S3: References

1. West, R. M.; Tucker, M. H.; Braden, D. J.; Dumesic, J. A., Production of alkanes from biomass derived carbohydrates on bi-functional catalysts employing niobium-based supports. **2009,** *10* (13), 1743-1746.
2. Buitrago-Sierra, R.; Serrano-Ruiz, J. C.; Rodríguez-Reinoso, F.; Sepúlveda-Escribano, A.; Dumesic, J. A., Ce promoted Pd–Nb catalysts for γ-valerolactone ring-opening and hydrogenation. *Green Chemistry* **2012,** *14* (12), 3318-3324.
3. Rouquerol, F.; Rouquerol, J.; Sing, K. S. W.; Llewellyn, P.; Maurin, G., *Adsorption by Powders and Porous Solids: Principles, Methodology and Applications*. 2nd ed.; 2014.
4. Georgacakis, D.; Dalis, D., Controlled anaerobic digestion of settled olive-oil wastewater. *Bioresource Technology* **1993,** *46* (3), 221-226.
5. Meyer, T.; Edwards, E. A., Anaerobic digestion of pulp and paper mill wastewater and sludge. *Water Research* **2014,** *65*, 321-349.
6. Davis, R. E.; Grundl, N. J.; Tao, L.; Biddy, M. J.; Tan, E. C.; Beckham, G. T.; Humbird, D.; Thompson, D. N.; Roni, M. S. *Process Design and Economics for the Conversion of Lignocellulosic Biomass to Hydrocarbon Fuels and Coproducts: 2018 Biochemical Design Case Update; Biochemical Deconstruction and Conversion of Biomass to Fuels and Products via Integrated Biorefinery Pathways*; United States, 2018-11-19, 2018.
7. Lee, J. M.; Upare, P. P.; Chang, J. S.; Hwang, Y. K.; Lee, J. H.; Hwang, D. W.; Hong, D. Y.; Lee, S. H.; Jeong, M. G.; Kim, Y. D.; Kwon, Y. U., Direct hydrogenation of biomass-derived butyric acid to n-butanol over a ruthenium-tin bimetallic catalyst. *ChemSusChem* **2014,** *7* (11), 2998-3001.
8. Dutta, A.; Sahir, A. H.; Tan, E.; Humbird, D.; Snowden-Swan, L. J.; Meyer, P. A.; Ross, J.; Sexton, D.; Yap, R.; Lukas, J. *Process Design and Economics for the Conversion of Lignocellulosic Biomass to Hydrocarbon Fuels: Thermochemical Research Pathways with In Situ and Ex Situ Upgrading of Fast Pyrolysis Vapors*; United States, 2015-03-01, 2015.
9. Humbird, D.; Davis, R.; Tao, L.; Kinchin, C.; Hsu, D.; Aden, A.; Schoen, P.; Lukas, J.; Olthof, B.; Worley, M.; Sexton, D.; Dudgeon, D. *Process Design and Economics for Biochemical Conversion of Lignocellulosic Biomass to Ethanol: Dilute-Acid Pretreatment and Enzymatic Hydrolysis of Corn Stover*; United States, 2011-03-01, 2011.
10. CatCost, a catalyst cost estimation tool, version 1.0.0; National Renewable Energy Lab: Golden, CO, USA, 2018; https://catcost.chemcatbio.org.11. Baddour, F. G.; Snowden-Swan, L.; Super, J. D.; Van Allsburg, K. M., Estimating Precommercial Heterogeneous Catalyst Price: A Simple Step-Based Method. *Organic Process Research & Development* **2018,** *22* (12), 1599-1605.